Functional Materials 15, No.2 (2008)

Control of radiation-conductive heat exchange at crystal growth from melt

V.I.Deshko, A.Ya.Karvatskii, A.V.Lenkin, Yu.V.Lokhmanets

National Technical University of Ukraine "Kiev Polytechnic Institute",
37, Pobedy Ave., 03056 Kyiv, Ukraine

Received July 09, 2007

The influence of radiation heat exchange in a crystal-melt system for different (from the point of view of optical properties) material classes and crystal growing methods (at constant crystal-melt system thickness and at a constant melt thickness) is considered. The general approach is based on using of modified numerical one-dimensional crystallization model at radiation-conductive heat exchange. The radiation heat transfer in a crystal-melt system provides conditions for faster front movement. In this case, most favorable conditions with large temperature gradients are created in systems with transparent crystal and opaque melt. At simultaneous crystal and melt "transparency" the temperature gradients in melt may decrease and cause stability loss of the directed crystallization.

Рассматривается влияние радиационного теплообмена в системе кристалл-расплав для разных с точки зрения оптических свойств классов материалов и методов выращивания кристаллов: при постоянной толщине системы кристалл-расплав и при постоянной толщине расплава. Общий подход построен на использовании модифицированной численной одномерной модели кристаллизации при радиационно-кондуктивном теплообмене. Радиационный теплоперенос в системе кристалл-расплав обеспечивает условия для более быстрого перемещения фронта, при этом наиболее благоприятные условия с большими градиентами температуры создаются в системах прозрачный кристалл - непрозрачный расплав. При одновременной "прозрачности" кристалла и расплава градиенты температуры в расплаве могут уменьшаться и приводить к потере устойчивости направленной кристаллизации.

Crystal growth from the melt can occur due to temperature field configuration change near to the crystallization front. In other methods, the crystal growth occurs by pulling from the melt. The motive power for the directed crystallization is the temperature gradient directed from crystal to melt. The considerable melt overheat can result in polycrystal growth, while overcooling, to dendritic one [1]. The temperature field formation in a crystal-melt system at the directed crystallization is one of the major conditions for growing of high-quality crystals.

Numerical models of heat exchange processes provide study and search for process control ways for crystal growth and reflect features both of various growth methods and for various materials [2-4]. An essential role of radiation heat transfer is always emphasized in high-temperature processes of crystallization from melt [4, 5], and the ways to its use for control of processes at the front are considered [6]. The purpose of this work is to study radiation heat exchange influence on thermal conditions in crystal-melt system for different (from the point of view of optical properties) materials classes and crystal growth methods. The general approach is based on using of modified numerical one-dimensional crystallization model at radiation-conductive heat exchange (RCHE) [5].

The various material types are modeled in the work : transparent crystal and melt (for example, halides); systems with increasing absorption, both in melt and in crystal; transparent crystal and opaque melt (oxides); opaque crystal and opaque melt (semiconductors). The attempt to generalize and compare the conditions for different

growth methods is connected with use of two crystals growth models: at constant thickness of the crystal-melt system and at a constant melt thickness.

Two semitransparent "gray" media are considered in the 1D model: a crystal and melt with temperature-independent thermophysical properties. The directed crystallization process starts from a stationary mode due to temperature decrease at a hot opaque boundary of the system and at a cold semitransparent boundary. The non-stationary T-field in a crystal ($k = \mathrm{cr}$) and melt ($k = \mathrm{m}$) at RCHE is described by the equation:

$$\rho_k c_k \frac{\partial T_k(x)}{\partial \tau} = \frac{\partial}{\partial x}\left(\lambda_k \frac{\partial T_k(x)}{\partial x}\right) - \frac{\partial q_k^{\mathrm{r}}(x)}{\partial x}, \tag{1}$$

where λ, c, ρ are heat conductivity, isobaric thermal capacity, and material density, respectively; τ, time; x, current coordinate; T, temperature.

The Stephan condition (the balance of energy at the front) at RCHE looks like:

$$Q_L \frac{dz}{d\tau} = \left(\lambda_{\mathrm{cr}} \frac{\partial T(x)}{\partial x}\bigg|_{z-} + q_{\mathrm{cr}}^{\mathrm{r}}\big|_{z-}\right) - \left(\lambda_{\mathrm{m}} \frac{\partial T(x)}{\partial x}\bigg|_{z+} + q_{\mathrm{m}}^{\mathrm{r}}\big|_{z+}\right), \tag{2}$$

where Q_L is the volume heat of the phase transititon; z, the front position.

Within the gap under the lower semi-transparent crystal boundary, the heat transfer is defined by the heat transfer coefficient besides of radiation. The influence of that gap on the radiation heat transfer in the system is set by pre-specification of the effective reflection coefficient at the boundary that takes into account the multiple reflection in the gap [7].

Radiation flux q^{r} and radiation flux divergence $\dfrac{\partial q^{\mathrm{r}}(x)}{\partial x}$ included into equations (1) and (2), are defined by heat radiation intensity in positive $I^+(x,\mu)$ and negative $I^-(x,\mu)$ directions and by radiation intensity of absolute black body $I_{\mathrm{b}}(x)$:

$$q_k^{\mathrm{r}}(x) = 2\pi \int_0^1 \left[I^+(x,\mu) - I^-(x,\mu)\right]\mu d\mu \tag{3},$$

$$\frac{\partial q_k^{\mathrm{r}}(x)}{\partial x} = -2\pi a_k \left(\int_0^1 \left[I^+(x,\mu) - I^-(x,\mu)\right]\mu d\mu - 2n_k^2 I_{\mathrm{b}}(x)\right), \tag{4}$$

where a is the absorption factor; n, refractive index; μ, cosine of angle between intensity vector and growth direction OX; $I_{\mathrm{b}}(x) = (\sigma/\pi)\mathrm{T}^4$, the black body radiation intensity in the specified point.

The radiation intensities $I^+(x,\mu)$ and $I^-(x,\mu)$ from equations (3) and (4), can be determined from the following equations (according to [7]):

$$\begin{cases} I^+(x,\mu) = I^+(0)\exp\left[-\dfrac{k_{\mathrm{cr}} x}{\mu}\right] + n_{\mathrm{cr}}^2 k_{\mathrm{cr}} \displaystyle\int_0^x \frac{I_{\mathrm{b}}(\eta)}{\mu}\exp\left[-\frac{k_{\mathrm{cr}}(x-\eta)}{\mu}\right]d\eta \\ I^-(x,\mu) = I^-(z^-)\exp\left[-\dfrac{k_{\mathrm{cr}}(z^- - x)}{\mu}\right] + n_{\mathrm{cr}}^2 k_{\mathrm{cr}} \displaystyle\int_x^{z^-} \frac{I_{\mathrm{b}}(\eta)}{\mu}\exp\left[-\frac{k_{\mathrm{cr}}(\eta - x)}{\mu}\right]d\eta \end{cases} \tag{5}$$

$$\begin{cases} I^+(x,\mu) = I^+(z^+)\exp\left[-\dfrac{k_{\mathrm{m}}(x - z^+)}{\mu}\right] + n_{\mathrm{m}}^2 k_{\mathrm{m}} \displaystyle\int_{z^+}^x \frac{I_{\mathrm{b}}(\eta)}{\mu}\exp\left[-\frac{k_{\mathrm{m}}(x-\eta)}{\mu}\right]d\eta \\ I^-(x,\mu) = I^-(L)\exp\left[-\dfrac{k_{\mathrm{m}}(L - x)}{\mu}\right] + n_{\mathrm{m}}^2 k_{\mathrm{m}} \displaystyle\int_x^L \frac{I_{\mathrm{b}}(\eta)}{\mu}\exp\left[-\frac{k_{\mathrm{m}}(\eta - x)}{\mu}\right]d\eta, \end{cases} \tag{6}$$

where η is the current coordinate along $0X$ axis. The equation (5) concerns the crystal phase, while (6), the melt. The first component in right-hand part of these equations describes the incident radiation in point x from the boundary of the phase considered, the second component is incident radiation from all internal phase layers positioned between the boundary and the current point.

The radiation intensities on external boundaries of the crystal-melt system $I^+(0)$, $I^-(L)$ and on the crystallization front $I^-(z^-)$, $I^+(z^+)$ can be determined from the radiation energy balance on the system boundaries. For a crystal, the equation system is following:

$$\begin{cases} I^+(0) = n_{\text{cr}}^2 (1 - R_{\text{cr}}) I_{\text{b}}(0) + 2R_{\text{cr}} \int_0^1 I^-(0,\mu)\mu d\mu \\ I^-(z^-) = 2R_{\text{cr-m}} \int_0^1 I^+(z^-,\mu)\mu d\mu + 2(1 - R_{\text{m-cr}}) \int_0^1 I^-(z^+,\mu)\mu d\mu . \end{cases} \tag{7}$$

In the first equation of system (7), the radiation intensity on the external crystal boundary is equal to sum of inherent boundary radiation and reflected radiation from all crystal layers. In the second equation, the radiation intensity on semitransparent crystallization front is sum of reflected radiation from the crystal side and radiation which coming from the melt through the interface. The radiation energy balance for the melt boundaries is written is similar manner:

$$\begin{cases} I^-(L) = n_{\text{m}}^2 (1 - R_{\text{m}}) I_{\text{b}}(T(L)) + 2R_{\text{m}} \int_0^1 I^+(L,\mu)\mu d\mu \\ I^+(z^+) = 2R_{\text{m-cr}} \int_0^1 I^-(z^+,\mu)\mu d\mu + 2(1 - R_{\text{cr-m}}) \int_0^1 I^+(z^-,\mu)\mu d\mu . \end{cases} \tag{8}$$

$R_{\text{cr}-\text{m}}$ in (7), (8) is the diffuse reflection coefficient of semitransparent interface from the crystal side, $R_{\text{m-cr}}$, that from the side of melt.

To obtain the equations for radiation heat flux and its divergence in each of the phases, it is necessary to solve the system of twelve equations, which consists of energy balance equations at the crystal and melt boundaries (7), (8), formal solutions of transfer equations written for current coordinate, (5) and (6), and formal solutions of the same equations written for the system boundaries, i.e. Eqs. (5) written for $x = z$ and $x = 0$, respectively, and Eqs. (6), for x=L and x=z.

The finite difference method is applied to T-field (1) calculation in each phase. The combined explicit-implicit scheme with use of dynamically rebuilded coordinate grid is applied for more exact definition of the front position and temperature conditions. The temperature linearization with use of Newton method is applied to solve the system of nonlinear equations (because of radiation component presence). The partial three-point linearization of radiation flows is carried out, that practically does not influence the convergence rate of iterative process and allows to keep the equation systems three-diagonally. The efficiency of 1D model was checked by comparison with literature data. The results have shown that the calculation error does not exceed 1 %.

A model material with thermophysical properties like BGO, crystallization temperature $T_0 = 1323$ K, was used in the studies. The crystallization versions in the crystal-melt system with different optical properties were considered, at various modes of system cooling, various temperature drops in crystal and melt. The calculations have shown that it is just radiation heat exchange that is the main heat transfer mechanism: the radiation part in the total heat transfer reaches 95%.

The results of stationary temperature distribution calculations in the crystal-melt system at different absorption factors of crystal and melt and identical total temperature drop in the system are shown in Fig. 1. Let the results for "transparent" crystal ($a_{\text{c}} = 3$ m^{-1}) be considered. The interface is in different temperature conditions at "transparent" melts ($a_{\text{m}} = 50$ m^{-1}) and for opaque melts ($a_{\text{m}} = 50000$ m^{-1}) crystallization, the boundary conditions

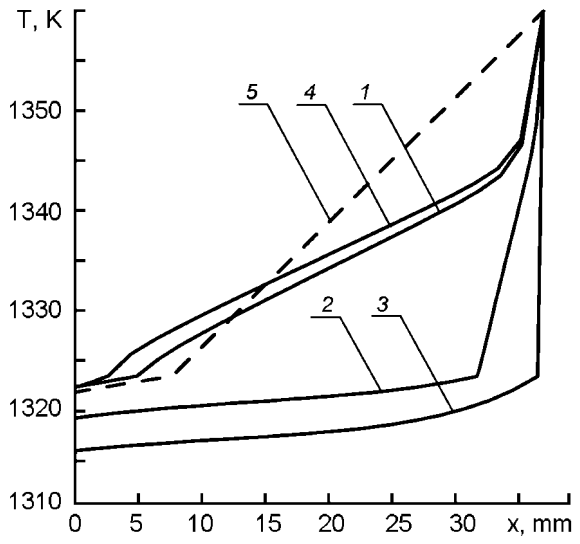

Fig. 1. Stationary temperature distribution in crystal-melt system at different crystal and melt absorption factors in m-1, accordingly: *1* – 3/50; *2* – 3/500; *3* – 3/50000; *4* – 50/50; *5* – 50000/50000; 50000 m-1 means opaque melt or crystal. The general temperature drop in the system is identical and equal 55 K.

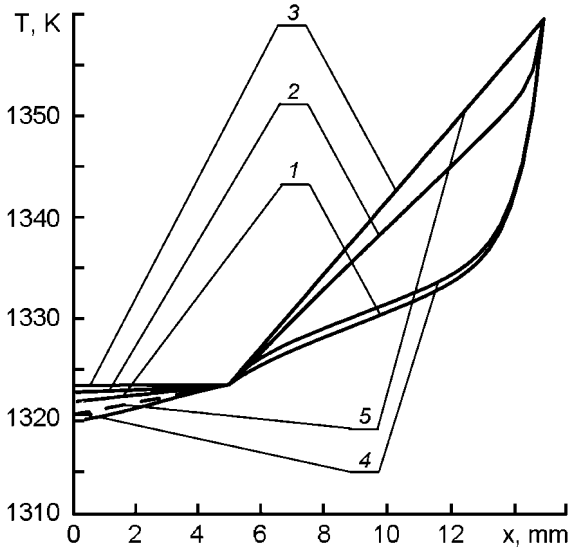

Fig. 2. Stationary temperature distribution in crystal-melt system at different crystal and melt absorption factors in m-1, accordingly: *1* – 3/50; *2* – 3/500; *3* – 3/50000; *4* – 50/50; *5* – 50000/50000; 50000 m-1 means opaque melt or crystal. The front position is identical.

being the same. At low absorption factors, the central melt zone radiation flows are more considerable as compared to the periphery and, accordingly, temperature gradients are smaller. As the melt absorption increases, the fraction of through fluxes at the front (which depend on the top boundary temperature) decreases, and radiation flows begin to depend on the temperature of melt layers near the front. Consequently, the crystal would be cooler, and the front is located more close to hot boundary. For opaque melt, the radiation flow to crystal is an essential component of energy balance at the front; therefore, the temperature gradient in melt is maximal.

Comparing the temperature distributions with identical absorption factors of the crystal and melt, it has been found that increasing system optical thickness results in more pronounced S-shape of temperature profile at first and, under the considered conditions, in some front displacement to the bottom boundary. In an opaque system, the temperature gradients ratio is defined by heat conductivity values for crystal and melt.

Taking into account the similar influence of absorption and radiation heat transfer, the front position sensitivity to temperature conditions change on boundaries was considered. For "transparent" system, the greatest influence on the front at its various positions is caused by hot boundary temperature change. For system with "transparent" crystal and opaque melt, on the contrary, the cold boundary influence is stronger. For pure conductive heat transfer, the stronger influence causes the border which is closer to the front position. Hereinafter, the starting conditions for the crystallization process analysis are chosen at identical position of front (fig. 2). For different absorption factors, this was reached by corresponding selection of cold boundary initial temperature.

The crystallization process was considered at identical temperature change rates at the system external boundaries. The calculations were carried out at various values of cooling rate and temperature drop. The temperature profiles at various time moments for "transparent" system are shown in Fig. 3, for system with "transparent" crystal - opaque melt, in Fig. 4. The front displacement in the central part of "transparent" system occurs in conditions of relatively low gradients, both in the crystal and in the melt, where an unstable directed crystallization zone [5] arises. To avoid the decrease of temperature gradients below the stability limit, the process should be carried out at a lower cooling rate. In a system with "transparent" crystal and opaque melt, the growth conditions arise with the large temperature gradients in melt, higher movement rate and stability. The front position variation for systems with various absorption characteristics is shown in Fig. 5, starting conditions see Fig. 2. The greatest front move-

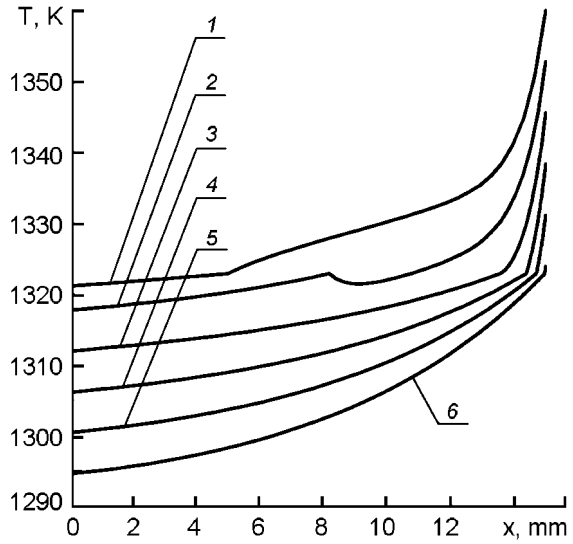

Fig. 3. Temperature field change in time: absorption factor for crystal is 3 m-1, for melt – 50 m-1, bounds cooling rate is 0.18 K/min.; time moments in minutes: *1* – 0; *2* –40; *3* –80; *4* – 120; *5* – 160; *6* – 200.

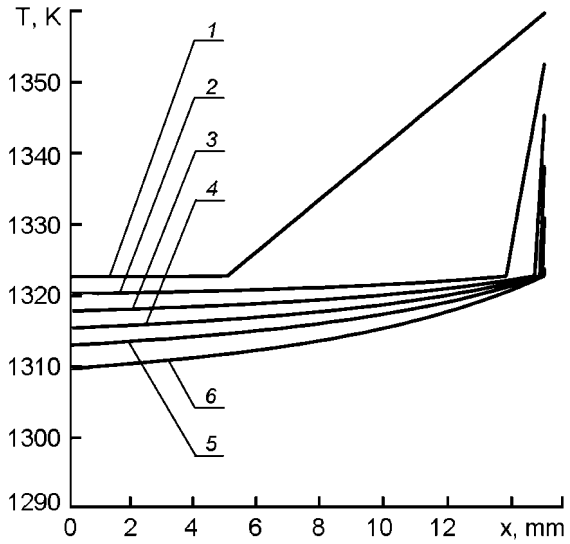

Fig. 4. Temperature field change in time: absorption factor for crystal is 3 m-1, for melt – 50000 m-1(opaque), bounds cooling rate is 0.18 K/min.; time moments in minutes: *1* – 0; *2* – 40; *3* –80; *4* – 120; *5* – 160; *6* –200.

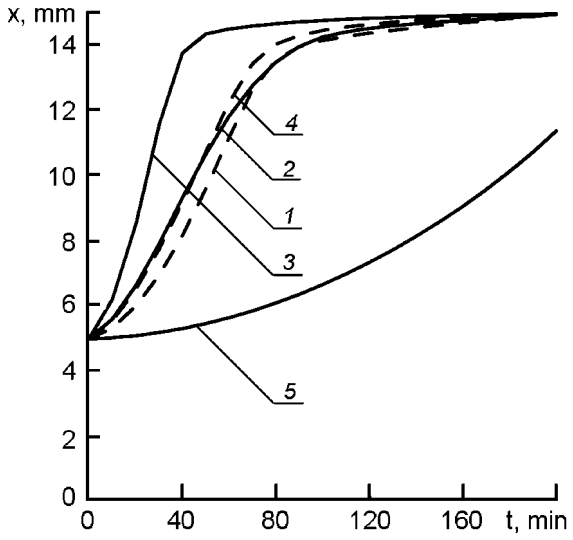

Fig. 5. Crystallization front position change at time at different crystal and melt absorption factors in m-1, accordingly: *1* – 3/50; *2* – 3/500; *3* – 3/50000; *4* – 50/50; *5* – 50000/50000; 50000 m-1 means opaque melt or crystal; bounds cooling rate is 0.18 K/min.

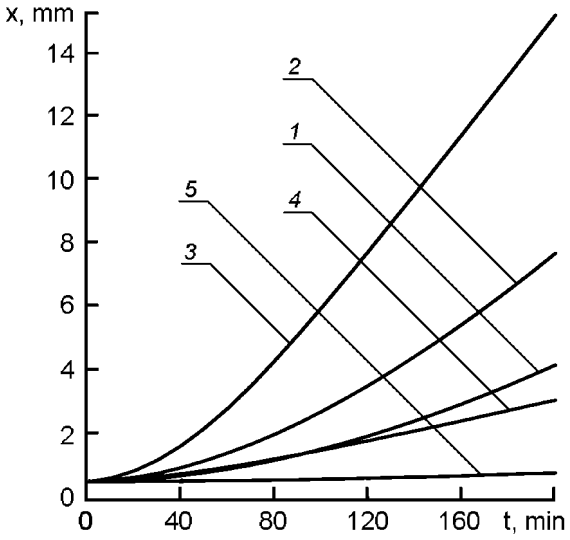

Fig. 6. Crystallization front position change at time at different crystal and melt absorption factors in m-1, accordingly: *1* – 3/50; *2* – 3/500; *3* – 3/50000; *4* – 50/50; *5* – 50000/50000; 50000 m-1 means opaque melt or crystal; the melt thickness is constant, cold bound cooling rate is 0.18 K/min.

ment rate is observed for system with "transparent" crystal and opaque melt where conditions of the maximum radiation heat removal from the front are provided. The least front movement takes place in opaque system. Decrease of the rate near to hot boundary is connected in all cases with temperature gradients increase in melt near the front. Similar trends in the front movement rate change are observed under starting conditions according to Fig. 1.

The non-stationary RCHE processes in a crystal-melt system have been calculated at cold boundary constant cooling rate only, starting conditions see Fig. 2. The results for system with "transparent" crystal and opaque melt practically coincide with the data considered before, received at simul-

taneous cooling of both boundaries. Under constancy of hot boundary temperature conditions, some front movement deceleration takes place on a final part of time interval set for systems with high absorption. The greatest process deceleration is caused by this factor in opaque system.

The model version has been developed where the melt feed is carried out from the hot boundary side in such a way that at crystal growth, the melt thickness and temperature drop therein are kept constant by the cooling of the crystal cold butt. The front position change for systems with various absorption characteristics under starting conditions of Fig. 2, as calculated using this model, is shown in Fig. 6. As well as in Fig. 5, the greatest front movement is registered for system with "transparent" crystal and opaque melt, and the least one, for a completely opaque system. At the same time, in systems with radiation heat transfer and constant melt thickness, the front movement rate can be 10 times more than in system with constant system thickness.

To conclude, the radiation heat transfer in a crystal-melt system provides conditions for faster front movement in comparison with systems with pure conductive heat transfer. In this case, most favorable conditions with large temperature gradients are developed in systems with opaque melt. At simultaneous crystal and melt "transparency", the temperature gradients in melt may decrease and result in stability loss of the directed crystallization. The considered features of thermal processes in crystal-melt system caused by radiation heat transfer influence are reasonable to take into account, along with data on kinetic conditions of growth, at optimization and new crystal growth processes development.

References

1. V.I.Goriletsky, B.V.Grinyov, B.G.Zaslavsky. Crystal Growth. Akta, Kharkiv (2002).
2. B.L.Timan, O.D.Kolotiy, in: Single Crystals and Engineering, 14th Issue, VNII Monocrystallov, Kharkiv (1976), p. 86.
3. A. Yeckel, A.Pandy, J.J.Derby, in: Advances in Computational Heat Transfer II, New York Academy of Sciences (2001), p. 1193.
4. S.Brandon, J.J.Derby, *J. Cryst. Growth, 110,* 481 (1991).
5. V.I. Deshko, A.Ya.Karvatskii, *Promyshlennaya Teplotekhnika 10*, 60 (1988).
6. V.I.Deshko, A.J.Karvatskii, A.V.Lenkin, in: Abstr. of IV Intern. Conf. on Problems of Industrial Heat Engineering, Sept 26–30, 2005, Kyiv, Ukraine (2005), p. 278.

Управління процесами радіаційно-кондуктивного теплообміну при кристалізації з розплаву

В.І. Дешко, А.Я. Карвацький, О.В. Ленькін, Ю.В. Лохманець

Розглядається вплив радіаційного теплообміну у системі кристал-розплав для різних з точки зору оптичних властивостей класів матеріалів і методів вирощування кристалів: при постійній товщині системи кристал-розплав і при постійній товщині розплаву. Загальний підхід оснований на використанні модифікованої чисельної одновимірної моделі кристалізації при радіаційно-кондуктивному теплообміні. Радіаційний теплоперенос у системі кристал-розплав забезпечує умови для швидшого переміщення фронту, при цьому найбільш сприятливі умови з великими градієнтами температури створюються у системах прозорий кристал - непрозорий розплав. При одночасній «прозорості» кристала і розплаву градієнти температури у розплаві можуть зменшуватися і приводити до втрати стабільності процесу направленої кристалізації.